REFERENCE ONLY

Sea-Surface Backscattering and the Soliton Mechanism

R. H. Mellen, D. Middleton, and J. W. Fitzgerald
(Consultants)

Associate Technical Director
for Technology

REFERENCE ONLY

Naval Underwater Systems Center
Newport, Rhode Island / New London, Connecticut

Preface

This document was prepared under Contract No. N66604-85-B097 by Planning Systems Incorporated, Marine Sciences Division, Suite B, Foss Building, 95 Trumbull Street, New London, CT 06320.

Reviewed and Approved: 21 February 1986

W A Van Winkle

W. A. Von Winkle
Associate Technical Director
for Technology

REPORT DOCUMENTATION PAGE

1a. REPORT SECURITY CLASSIFICATION UNCLASSIFIED	1b. RESTRICTIVE MARKINGS
2a. SECURITY CLASSIFICATION AUTHORITY	3. DISTRIBUTION/AVAILABILITY OF REPORT Approved for public release; distribution unlimited.
2b. DECLASSIFICATION/DOWNGRADING SCHEDULE	

4. PERFORMING ORGANIZATION REPORT NUMBER(S) TD 7583	5. MONITORING ORGANIZATION REPORT NUMBER(S)

6a. NAME OF PERFORMING ORGANIZATION Naval Underwater Systems Center	6b. OFFICE SYMBOL (If applicable)	7a. NAME OF MONITORING ORGANIZATION
6c. ADDRESS (City, State, and ZIP Code) New London Laboratory New London, Connecticut 06320		7b. ADDRESS (City, State, and ZIP Code)

8a. NAME OF FUNDING/SPONSORING ORGANIZATION	8b. OFFICE SYMBOL (If applicable)	9. PROCUREMENT INSTRUMENT IDENTIFICATION NUMBER Contract No. N66604-85-B097

8c. ADDRESS (City, State, and ZIP Code)	10. SOURCE OF FUNDING NUMBERS			
	PROGRAM ELEMENT NO.	PROJECT NO.	TASK NO.	WORK UNIT ACCESSION NO.

11. TITLE (Include Security Classification)
SEA-SURFACE BACKSCATTERING AND THE SOLITON MECHANISM

12. PERSONAL AUTHOR(S)
R. H. Mellen, D. Middleton, and J. W. Fitzgerald

13a. TYPE OF REPORT	13b. TIME COVERED FROM ____ TO ____	14. DATE OF REPORT (Year, Month, Day) 1986, February 21	15. PAGE COUNT

16. SUPPLEMENTARY NOTATION

17.	COSATI CODES		18. SUBJECT TERMS (Continue on reverse if necessary and identify by block number)
FIELD	GROUP	SUB-GROUP	

19. ABSTRACT (Continue on reverse if necessary and identify by block number)

Sonar and radar measurements both indicate that there are fundamental problems with the present wind-wave models of the sea surface at higher wavenumbers; i.e., backscattering strengths at high frequencies and small grazing angles are much greater than predicted and the Doppler spectra show no evidence of the dispersion expected in the gravity-capillary regime. Quasi-linear wave theories do not account for these effects.

Laboratory wind-wave flume measurements also support this conclusion. Photographs reveal that wavefronts of ripples tend to steepen with increasing fetch. Spectra of wave-gauge data also show a corresponding growth of coherent harmonics. Nonlinear amplitude effects can account for the non-dispersive behavior of waves in this regime.

With further increase in fetch, the wave-gauge data also show the growth of sub-harmonics followed by rapid degeneration to a continuous spectrum. This suggests that a

20. DISTRIBUTION/AVAILABILITY OF ABSTRACT ☐ UNCLASSIFIED/UNLIMITED ☒ SAME AS RPT. ☐ DTIC USERS	21. ABSTRACT SECURITY CLASSIFICATION UNCLASSIFIED	
22a. NAME OF RESPONSIBLE INDIVIDUAL	22b. TELEPHONE (Include Area Code)	22c. OFFICE SYMBOL

DD FORM 1473, 84 MAR

83 APR edition may be used until exhausted.
All other editions are obsolete.

19. (Cont'd)

second mechanism is involved in sea-state development; namely, chaotic behavior arising from surface-instability and wave-wind interaction.

A qualitative 4-stage model for wave growth is proposed:

a. Initiation of high-frequency surface ripples (catspaws) by the wind.

b. Nonlinear formation of steep wavefronts.

c. Generation of low-frequency waves by surface instability and wave-wind interaction.

d. Continued generation of unstable surface-disturbances which degenerate into ensembles of solitons, with incoming energy balanced by dissipation.

With assumptions not contrary to any of the known properties of the sea-surface, quantitative scattering predictions of the model are in good agreement with experiment re. backscattering strength and Doppler shift and spread in known bubble-free regimes. These results provide inferential support for the proposed sea-surface and scattering models. However, a program is needed for explicit verification of the model by direct observation and testing against more refined measurements of wave statistics and hydro-dynamic theory. Such a program proposal is outlined here.

The proposed program could have far-reaching implications. The primary goal is to predict sonar and radar scattering phenomena in total detail from knowledge of surface-wave statistics; however, the study reveals a potential "chaotic" mechanism for wave generation that could be crucial to developing a more comprehensive predictive model of sea-state development.

Planning Systems Incorporated

Marine Sciences Division
Suite B - Foss Building ■ 95 Trumbull Street ■ New London, CT 06320
(203) 447-3552

SEA-SURFACE BACKSCATTERING AND THE SOLITON MECHANISM

A Technical Review

FINAL REPORT
Prepared under:
NUSC Contract #N 66604-85-B097

Prepared by:

R. H. Mellen, D. Middleton & J. W. Fitzgerald

Prepared for:
Dr. W. A. Von Winkle
Code 10

U. S. Naval Underwater Systems Center
New London Laboratory
New London, CT 06320

30 September 1985

TABLE OF CONTENTS

ABSTRACT

Sonar and radar measurements both indicate that there are fundamental problems with the present wind-wave models of the sea surface at higher wavenumbers; i.e. backscattering strengths at high frequencies and small grazing angles are much greater than predicted and the Doppler spectra show no evidence of the dispersion expected in the gravity-capillary regime. Quasi-linear wave theories do not account for these effects.

Laboratory wind-wave flume measurements also support this conclusion. Photographs reveal that wavefronts of ripples tend to steepen with increasing fetch. Spectra of wave-gauge data also show a corresponding growth of coherent harmonics. Nonlinear amplitude effects can account for the non-dispersive behavior of waves in this regime.

With further increase in fetch, the wave-gauge data also show the growth of sub-harmonics followed by rapid degeneration to a continuous spectrum. This suggests that a second mechanism is involved in sea-state development; namely, chaotic behavior arising from surface-instability and wave-wind interaction.

A qualitative 4-stage model for wave growth is proposed:
a. Initiation of high-frequency surface ripples (catspaws) by the wind.
b. Nonlinear formation of steep wavefronts.
c. Generation of low-frequency waves by surface instability and wave-wind interaction.
d. Continued generation of unstable surface-disturbances which degenerate into ensembles of solitons, with incoming energy balanced by dissipation.

With assumptions not contrary to any of the known properties of the sea-surface, quantitative scattering predictions of the model are in good agreement with experiment re. backscattering strength and Doppler shift and spread in known bubble-free regimes. These results provide inferential support for the proposed sea-surface and scattering models. However, a program is needed for explicit verification of the model by direct observation and testing against more refined measurements of wave statistics and hydrodynamic theory. Such a program proposal is outlined here.

The proposed program could have far-reaching implications. The primary goal is to predict sonar and radar scattering phenomena in total detail from knowledge of surface-wave statistics; however, the study reveals a potential "chaotic" mechanism for wave generation that could be crucial to developing a more comprehensive predictive model of sea-state development.

LIST OF ILLUSTRATIONS

Figure   page

LIST OF SYMBOLS

c=soliton propagation speed

c_0=shallow-water wavespeed

C=surface-wave phase-speed

C_0=sound speed in water

d=effective depth of surface drift-layer

f=acoustic frequency

Δf=Doppler shift

$\underline{\Delta f}$=Doppler spread

F=surface-wave frequency

g=gravity constant

$G_2(K)$=2-dimensional surface-wave wavenumber spectrum

h=soliton vertical displacement

H=soliton ensemble rms height

H_0=soliton peak height

H_w=characteristic surface-wave rms height

$k=2\pi f/C_0$=acoustic wavenumber

$K=2\pi F/C$=surface wavenumber

K_0=characteristic soliton wavenumber

L=soliton ensemble rms wavelength or correlation length

L_0=characteristic soliton wavelength

$N(\theta,\emptyset)$=surface-wave backscattering tilt-factor

R=surface-wave scattering reflection-coefficient

$R=kH\sin\emptyset$=Rayleigh-roughness parameter

S^2= variance of surface-slopes

s^2="effective" variance of surface-slopes

T=specific surface-tension

U_c=surface-current speed

U_0=speed of drift-layer at the surface

U_∞=mean wind-speed

x=surface-wave fetch

$\emptyset$=acoustic grazing-angle

θ=acoustic azimuthal angle (Fig. 2A)

θ_c=surface-current angle (Fig. 2A)

Ω=characteristic surface-wave angular-frequency

1. INTRODUCTION

It has been widely observed, in both sonar and radar measurements at short wavelengths, that backscattering from ocean waves is generally much greater than predicted by classical models[1-12]. For wind speeds in the range 5-15 m/s, and grazing angles of 20° or less, the excess can amount to 15-20 dB even for the classical composite-surface backscattering models. The effect is particularly clear for underwater acoustics at frequencies above 10 kHz [1,2,9,11] and, for the EM case, at X-band, as the recent results of de Loor [11] and Lawner and Moore [12] indicate.

In the EM case, spray is often cited as a possible cause of enhanced backscattering-levels. In most underwater acoustic cases, a sub-surface bubble-layer created by breaking waves is assumed to be responsible [7-10]. However, recent very-precise experiments by Roderick et. al. [3] show that high levels can occur even without observable bubbles.

Various theories and approximations used in the analysis of backscattering data have been found to yield nearly the same results [1]. The observed discrepencies are, therefore, attributable to the choice of sea-surface models. Most of these are not at all specific as to behavior in the high-wavenumber regime.

A plausible surface mechanism has been advanced [1,2,4-6] that can potentially account for both the high backscattering-levels and the associated Doppler-shifts and spreads. The mechanism involves an ensemble of solitons or "hydraulic bumps" [13,14], produced as a consequence of nonlinear effects of <u>surface-drift</u> and <u>wave-wind</u> interactions.

The drift current develops through wind-drag and forms an effective surface-layer of the order of mm's in thickness with a surface speed of the order of 2-4% of the wind-speed [15]. The nonlinear effects of the layer cause steepening of the surface-waves, similar to breaking-wave phenomena in shallow water except that surface tension prevents "whitecap" formation in this case. Wave-gauge spectra show the development of harmonics of the ripple frequency with increasing fetch [16]. They also show growth of low-frequency waves. Wave-wind interaction is believed to be the result of developing surface-instability, which then becomes the principal mechanism for the generation of low-frequency waves.

In the equilibrium state, further surface disturbances generated by the wind will not be stable and will degenerate into soliton components. Accordingly, the scattering interface postulated here is not artificially divided into "gravity" and "capillary" components as in quasi-linear theory.

Soliton "ripples" are, therefore, a truly additional component of surface-roughness at higher wavenumbers. They ride on the moving gravity-capillary system and are responsible for backscattering at small grazing-angles and high frequencies [1,2,4].

It is evident that the wave spectra cannot be saturated at higher wavenumbers as it is in the low-wavenumber "gravity" regime. This has been amply demonstrated in both backscattering and wave-gauge experiments [17-19]. Indeed, the data suggest that mean wind speed U_∞ and fetch are not adequate parameters for defining sea-state and other factors, e.g. turbulence, higher moments of U_∞ may be important.

However, in addition to variations in spectrum level, there are other even more diagnostic scattering phenomena, i.e. Doppler shift and spread. Summary arguments for the soliton model are that:

1. The basic interaction mechanism of energy transfer is nonlinear and occurs primarily at high wavenumbers and the reverse cascade to lower wavenumbers evidently occurs through instability.
2. Solitons propagate at almost constant speed due to balance between dispersion and nonlinear amplitude effects of surface drift and are relatively unaffected by surface instability.
3. The observed Doppler properties are consistent with non-dispersive propagation of the soliton ensembles [2].
4. The existence of the additional soliton-ensemble component of roughness accounts for the higher backscattering strengths [2,4-6].

The preliminary nature of the experimental and theoretical knowledge here must be emphasized. Although the plausibility and general consistency of the model have been indicated, the detailed behavior or, in fact, even the existence of the soliton-ensemble has not yet been directly established. Thus far, all properties have been inferred from various experimental data and further direct verification is required. Accordingly, the purposes of this Technical Review are:

1. To provide a scientific and technical basis for a program to verify the existence and parametric dependence of the soliton ensemble on the wind-driven sea surface.
2. To determine the nature of any experiments required.
3. To suggest further theoretical investigations of the soliton model.
4. To correlate results of theoretical and experimental studies.
5. To provide an initial summary of the expected implications for the Navy, oceanography community, etc.

2. BACKGROUND

Extensive experimental evidence for the soliton scattering mechanism already exists in the open literature and will be reviewed here.
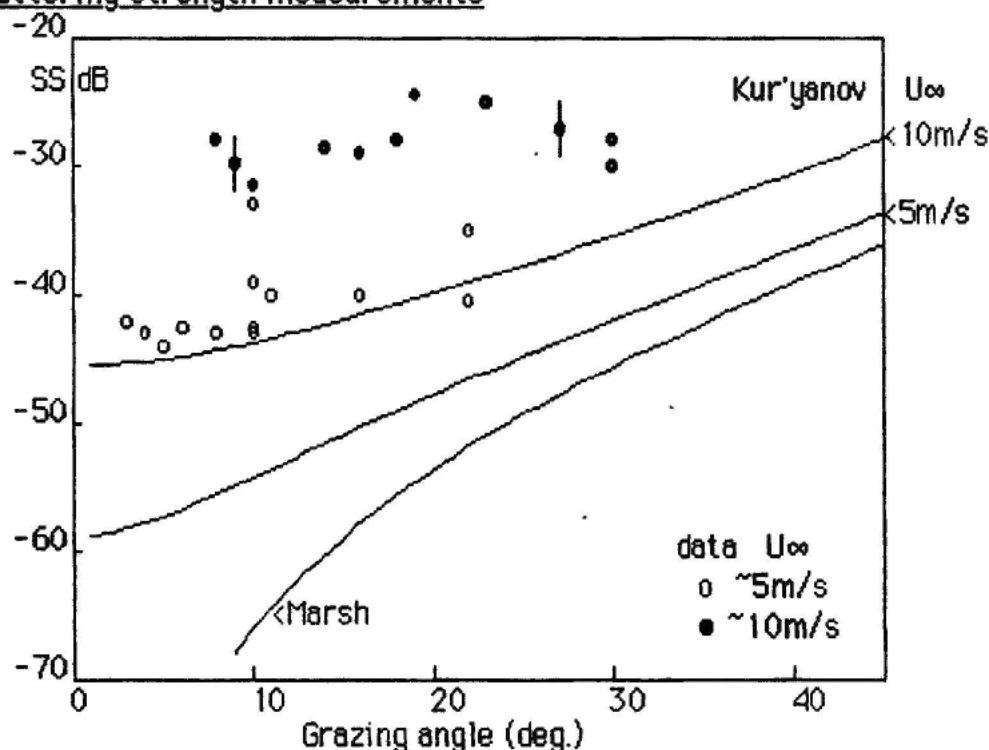
2.1. Scattering strength measurements

Figure 1: Backscatter models and data.

In 1963, Marsh [20] applied his scattering theory to the wave-spectrum model of Phillips [21]. For moderate mean wind-speeds, the spectrum becomes saturated at high wave-frequencies. Backscattering involves Bragg or "grating" resonance ($K=2k \cos\emptyset$) and the strength is proportional to $(k \tan\emptyset)^4$ where $\emptyset$ is grazing angle and k is the acoustic wavenumber. For a wavenumber K spectrum with constant K^{-4} asymptote, the backscattering strength formula becomes simply: $SS= -36+ 40\log(\tan\emptyset)$ dB.

The data of Figure 1 with error bars are from the parametric sonar measurements of Roderick et. al. [3] (9°, 5-20 kHz) and Lake Seneca measurements of Konrad et. al. [22] (30°, 250 kHz). All other data are from Urick [23], (60 kHz). Clearly, the Marsh formula predictions are too low.

To account for the discrepencies at small grazing angles, Kur'yanov [24] proposed a composite-roughness model in which the small-scale scatterers ride on the bigger waves. The local grazing angles then depend on the sea-state and the average value is increased accordingly. However, Kur'yanov's predictions are still 10-15 dB too low.

-3-

2.2 Doppler experiments

Anomalous behavior of surface waves was also observed in the Doppler spectra. According to theory, the CW backscatter spectrum from a narrow acoustic beam should have sharp spectral lines corresponding to Bragg resonance. The dispersion relation for phase speed C is given by $C^2=TK+g/K$ where g is gravity and T is surface tension. This relation was expected to hold over the entire surface-wave spectrum. However, experiment did not support the argument. Instead of the predicted sharp line, a broad peak was observed with a Doppler shift quite different from the predicted value.
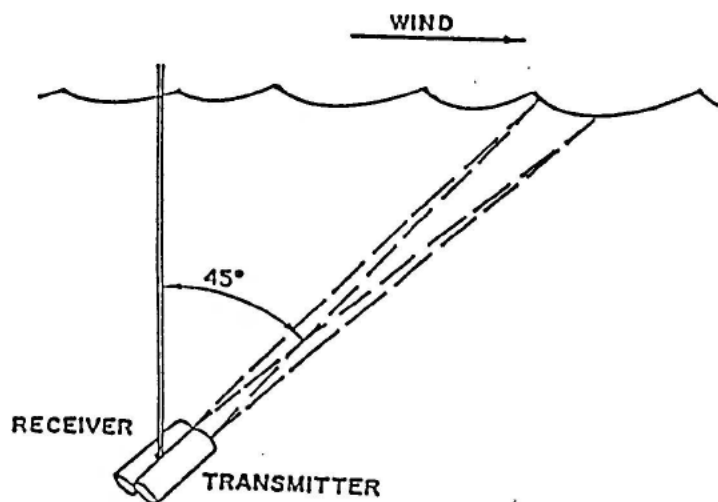

Figure 2: Experimental arrangement (ref. 25)

A Doppler experiment in the Thames River by Mellen [25] in 1963, is illustrated in Figure 2. In this experiment, the operating frequencies were 85 kHz and 1400 kHz, corresponding to resonance with the surface wavenumbers 5/cm and 40/cm respectively for the grazing angle 45°. The CW signal, backscattered from the illuminated surface, was band-shifted for spectrum analysis and the results plotted as a function of Doppler shift Δf from the carrier frequency f (Figures 3 and 4). The expected Doppler-shift is given by $\Delta f=2f\cos\emptyset\ C/C_0$ where C_0 is the sound-speed.

The mean wind-speed for the experiment was estimated to be 10 m/s. Although a few "whitecaps" were noted, there was no evidence of any significant entrapment of air. Pulse measurements showed no sub-surface return; therefore, the observations are believed to be indicative of purely surface-wave phenomena and not bubbles.
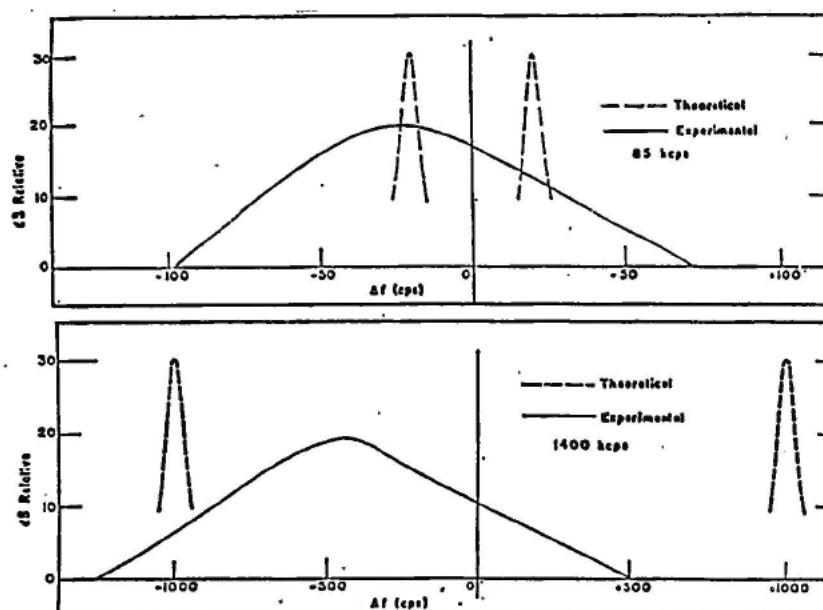
Figure 3: Doppler spectra (ref.25)

Figure 3 compares the measured Doppler spectra with the expected resonances indicated by the dashed lines. Negative shift corresponds to the downwind conditions of the experiment. Much of the Doppler spread can be attributed to modulation by the larger gravity waves; however, the Doppler shift at 1400 kHz is much too small.
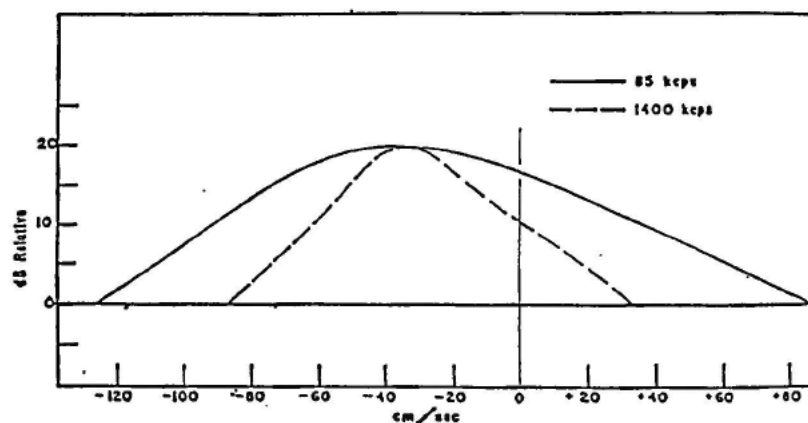

Figure 4: Phase-speed spectra (ref.25).

In Figure 4, the spectra are scaled according to apparent phase-speed. Both spectral peaks then coincide at approximately -35 cm/sec and this indicates that the scatterers are traveling non-dispersively.
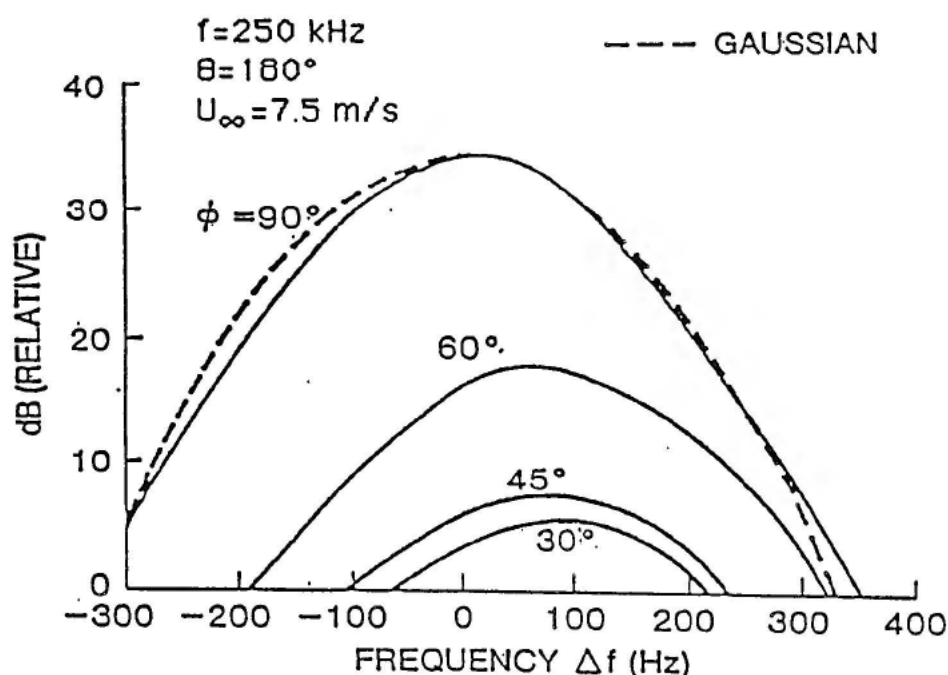
-5-

Figure 5: Doppler spectra vs grazing angle (ref. 22)

The Doppler spectra of the Lake Seneca experiments by Konrad et.al. [22], Figure 5, illustrate the effect of grazing angle looking upwind. The relative speed of the scatterers varies as $C \cos\emptyset$ and the peak of the spectrum shifts upward by an amount corresponding to $C \approx 35$ cm/s.

Normal to the surface ($\emptyset=90°$), the spectrum becomes symmetric about zero and is very close to Gaussian. This is characteristic of gravity waves and modulation of the scatterers by gravity wave motion must be the dominant factor in spectral spreading. Calculations show that essentially all of the Doppler spread is accounted for by this mechanism. The dominant surface-wave angular frequency was estimated to be $\Omega \approx 3$/sec. At $\emptyset=90°$, the Doppler spread around zero for the rms waveheight $H_w \approx 10$ cm is then

$\underline{\Delta f} = 2 f \Omega H_w / C_0 \approx \pm 100$ Hz, which is in good agreement with experiment.

The shift of the spectral peak with angle is consistent with propagation of the scatterers in the downwind direction independently of the motion of the gravity waves on which they ride. The average downwind speed is approximately 35 cm/sec. Some variability of both speed and direction of propagation is to be expected but the effect on spectral spreading at large grazing angles should be small.
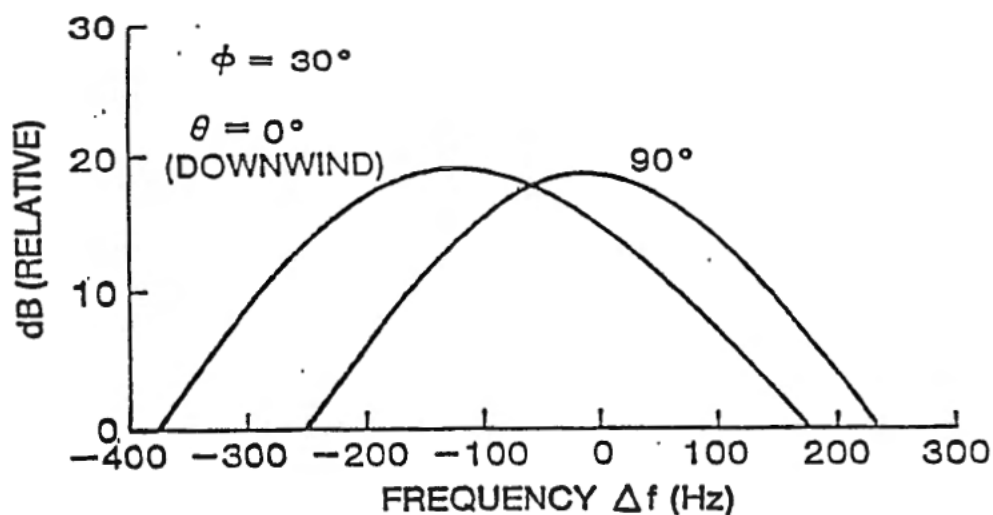
Figure 6: Doppler spectra vs azimuthal angle (ref.22).

Variation of angle with respect to wind direction also shifts the spectral peak as seen in Figure 6. Crosswind, the spectrum is symmetrical around zero as expected for the orbital motion of gravity waves.
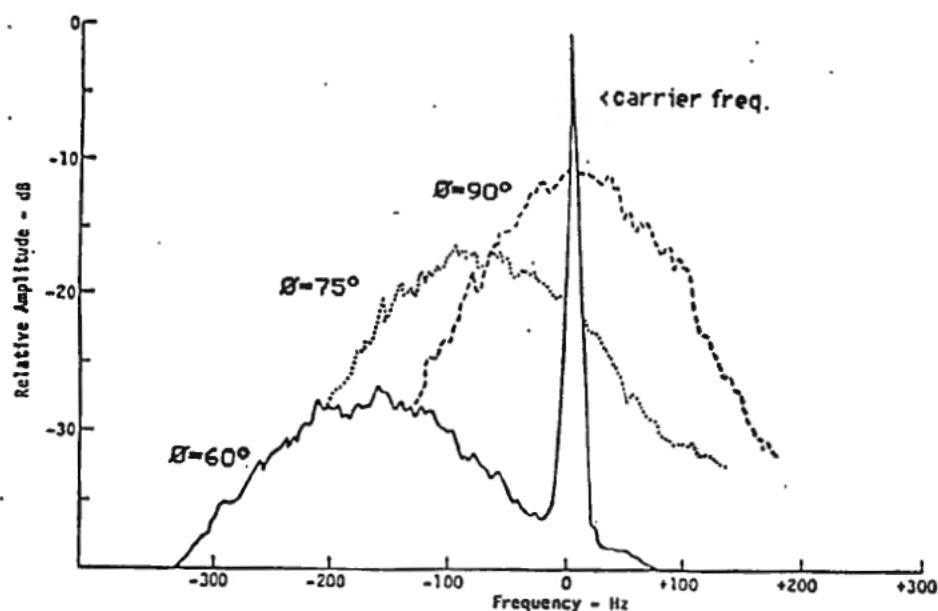

Figure 7: Doppler spectra vs grazing angle (ref. 26).

Figure 7 shows similar effects observed by Boehme [26] in the Lake Travis experiments looking downwind at the frequency 455 kHz with mean wind-speed 4 m/sec. The asymmetry of the spectrum indicates a velocity of ~50 cm/sec, which is significantly greater than the other results.

2.3 Tank experiments
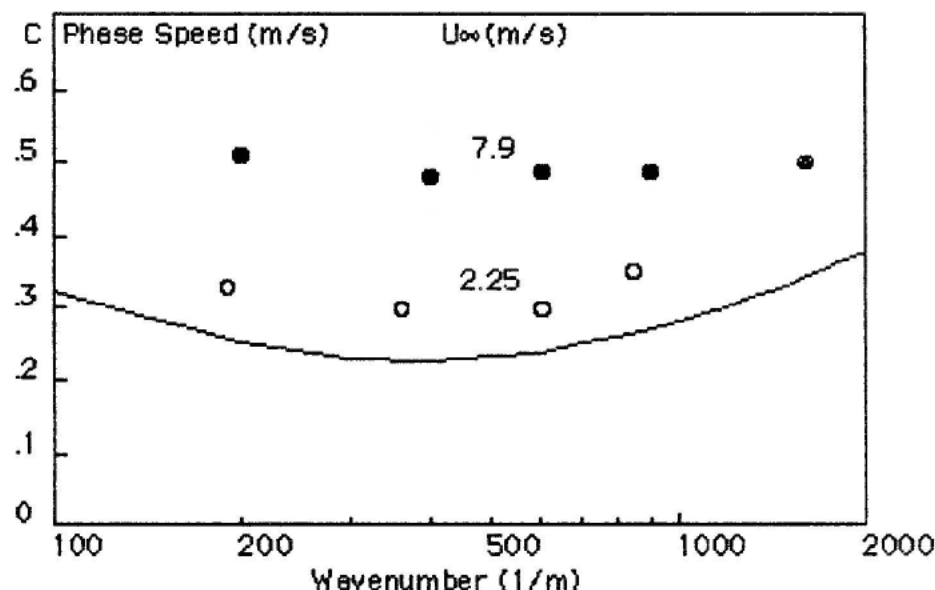
Figure 8: Phase-speed vs wavenumber (ref. 27)

In ripple-tank experiments, Wright and Keller [27] used a wave-gauge to measure effects of wind on the phase-speed of mechanically-generated surface-waves. Figure 8 compares the dispersion formula (solid line) with data which show negligible dispersion at high wind-speeds.

Figure 9: Phase-speed measurements (ref.16)

Wave-gauge measurements were also made by Ramamonjiarisoa et. al. [16] in a large wind-wave flume. Figure 9 shows a typical phase-speed data compared to theory (solid line). Dispersion is evident only below 3 Hz.

- 8 -

Figure 10: Wave spectra vs fetch (ref. 16)

In addition, frequency-spectrum measurements were made as a function of fetch. The spectra are sketched in Figure 10.

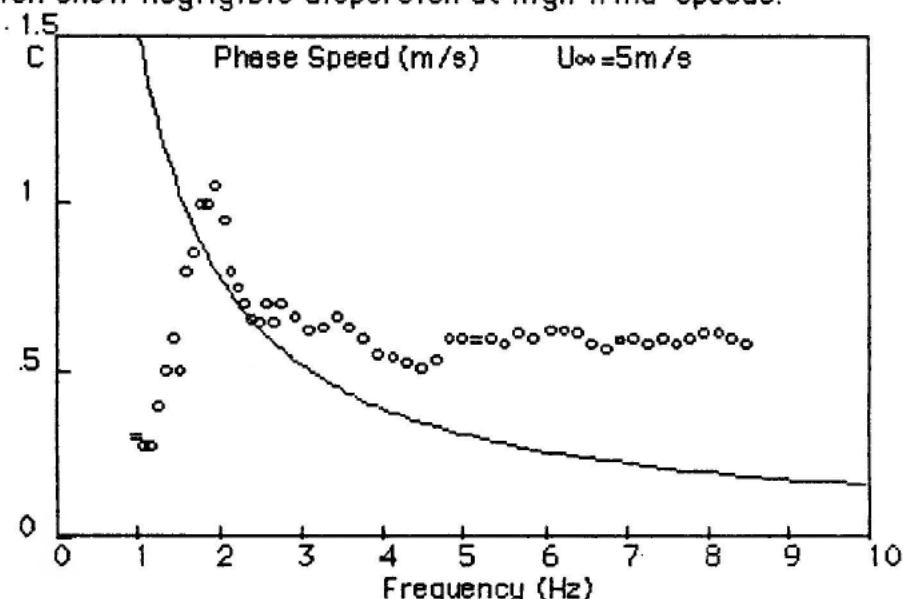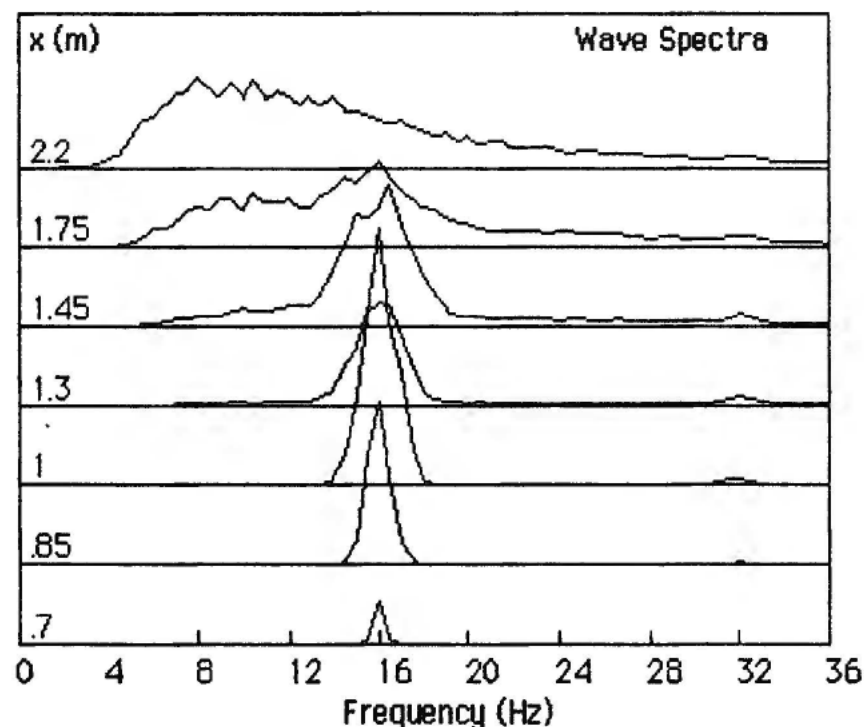For very short fetch x, the frequency-spectrum shows a single line near 16 Hz which increases in amplitude up to 1 m fetch. This is consistent with highly-periodic ripples (catspaws). The fronts of these ripples evidently tend to steepen and the spectrum at 1 m shows a clear harmonic at 32 Hz, which is expected for such a distorted waveform. In this regime, the cascade of energy is clearly toward higher frequencies. However, the 16 Hz line no longer increases in amplitude beyond 1 m. Instead it broadens and lower-frequency energy begins to appear below 16 Hz. This indicates that there must be a cascade of energy in the reverse direction as well.

A chaotic process is a plausible explanation for the generation of big waves by little ones. In the initial phase, one would expect to see a weak sub-harmonic at exactly half the ripple-frequency, i.e. 8 Hz; however, rapid degeneration of the system can cause broadening of both the sub-harmonic and the 16 Hz fundamental. As the wave grows and the amplitude reaches a critical point, the surface probably becomes unstable, destroying all the initial periodicity. This would explain the continuous spectrum seen at 2.2 m fetch.
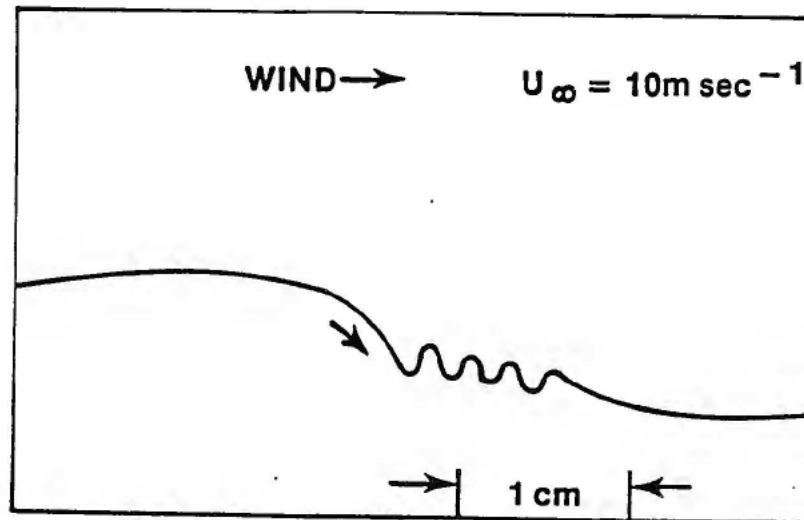
- 9 -

Figure 11: Surface waveform (ref. 28)

At short fetch, the ripple waveform simply becomes distorted. Figure 11 is a sketch of a typical waveform photograph made in a small tank by Schooley [28] for a mean wind-speed of 10 m/sec. In this stage, the ripples are highly periodic and only one cycle of the continuous wavetrain is displayed.

The waveform illustrates the typical distortion caused by nonlinear steepening. The arrow at the front indicates the direction of water-flow. The shock-like wavefront is also preceded by a small "capillary" ripple. This phenomenon can be readily observed in small tidal-pools under conditions of high wind.; however the effects then are due to shallow water, which is not the case above.

Growth of steep wavefronts requires some type of nonlinear amplitude effect. The waveform of Figure 11 is clearly similar to gravity waves in shallow water where the bottom causes an overtaking effect that can eventually lead to breaking. However, in the case of small-scale waves, capillary attraction is evidently sufficient to keep the wave from actually breaking. Banner and Phillips [29] refer to this phenomenon as "micro-breaking" and point out its significant role in the exchange of momentum between wave and wind.
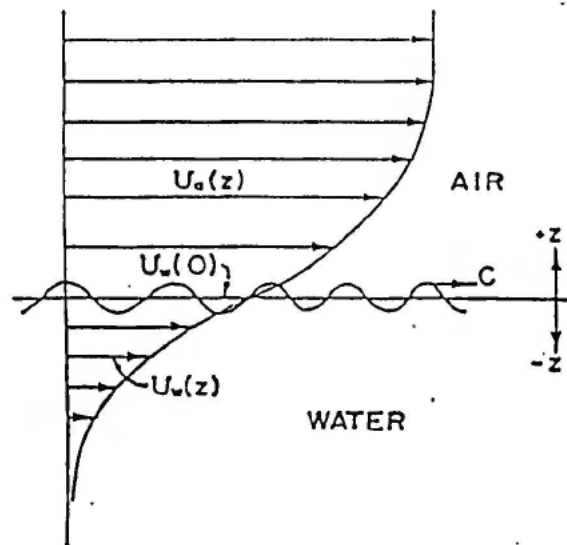
- 10 -

Figure 12: Drift-layer (ref. 15)

Shemdin [15] proposed surface-drift, illustrated in Figure 12, as the most likely nonlinear mechanism. Just as gravity waves steepen when they feel the bottom, waves travelling on a moving water layer steepen when they feel the effects of the slower water below. The drift layer can be approximated by an exponential decaying current with peak magnitude about 2-4% of wind-speed and of the order of mm's in thickness.

Nonlinear waves in a periodic system evidently encounter a potential well that stalls the advance of small-scale disturbances at the wavefront. A periodic steep-fronted wave consists of harmonics of the fundamental. Their growth involves a cascade of energy to higher wavenumbers and this does not explain how the sea develops.

Transfer of energy from wind to surface waves is, evidently, a high-wavenumber phenomenon. A second mechanism, involving a cascade of energy in the reverse direction, is needed to explain the generation of low-wavenumber energy. The most likely mechanism appears to be a similar transfer between the surface waves and the wind. Wave motion can no longer be considered "free" if it modulates the wind-force that generates it. Initially, this type of feedback will produce sub-harmonics. However, if the surface becomes unstable in the process, all periodicity will disappear and the wave motion will become chaotic. Transfer of energy from higher to lower wavenumbers is typical of chaotic systems.

3. SURFACE WAVE MODEL and SCATTERING EVIDENCE
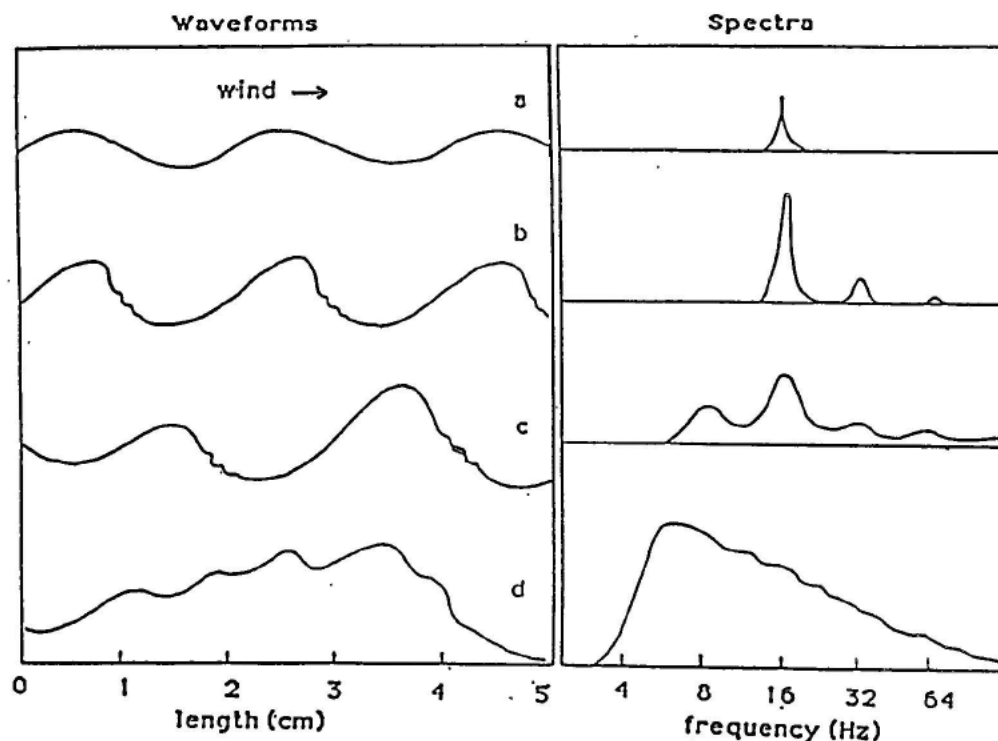
Figure 13: Wind-driven sea surface model (ref. 4)

The qualitative model of the build-up of the wind-driven sea, proposed by Middleton and Mellen [4], is illustrated in Figure 13. The four stages of wave development are:

a. Initiation of linear periodic ripples (catspaws) at 16 Hz near the frequency of minimum phase-speed.

b. Development of surface-drift causing nonlinear steepening of the wavefronts. Propagation speed increases without dispersion. Cascade of energy is toward higher wavenumbers.

c. Intermodulation between wind and water waves due to surface instability. Destruction of periodicity resulting in cascade of energy to lower wavenumbers.

d. Final equilibrium state. Growth of longer gravity waves ceases because they travel faster and outrun their source. Smaller disturbances, continually generated on the surface, are no longer stable and decompose into hydraulic "bumps" or solitons. Incoming wind energy is finally balanced by dissipation and the surface remains in equilibrium with continual development and decay of solitons

- 12 -

After the wave-wind interactions are sufficiently well-developed, small-scale disturbances generated on the surface have no periodic "potential wells" to trap them. Because of the resulting instability, they will decompose into elemental solitons or hyrdraulic "bumps" with specific amplitude and length relationships. The surface-drift layer provides a nonlinear balance, so that individual solitons propagate non-dispersively. The theory will be briefly summarized (see Appendix A). Viscosity will be neglected, although it will be an important effect in the later equilibrium stage. Surface-tension effects are minor at this order of approximation and will also be neglected.

From shallow-water wave theory, the equation for phase speed is:

$$C = c_0 \left[(\tanh(Kd)/(Kd)) \right]^{1/2} \approx c_0 (1 - (Kd)^2/6) \qquad c_0 \approx (gd)^{1/2}$$

where K is wavenumber, g is gravity and d is the depth. For solitons on the drift layer, the effective thickness d is taken as the U_0/e point.

Nonlinear effects can be approximated analytically in terms of "excess" wave-speed v by the Korteweg-de Vries (KdV) equation [13,14]:

$$v_t + (c_0 + v)v_x + A_0 v_{xxx} = 0 \qquad A_0 \approx c_0 d^2/6.$$

where subscripts indicate derivation with respect to the variables.

Solutions of the KdV equation are periodic "cnoidal" waves look like distorted sinusoidal waves as a consequence of the nonlinear second term. The governing parameter is $K_0 H_0/(K_0 d)^3$ where K_0 is wavenumber and H_0 is peak amplitude. As the value of the parameter increases, the wave period becomes longer and the waves tend to become solitary "bumps" or solitons. In the limiting case, the solution for the single isolated "bump" is given by:

$$v = 3 v_0 \operatorname{sech}^2[K_0(x-ct)], \quad c = c_0 + v_0, \quad K_0 = (3v_0/2c_0)^{1/2}/d.$$

Surface displacement is given by $h \approx 2v/3K_0 c_0$ and the waveform becomes:

$$h \approx H_0 \operatorname{sech}^2[K_0(x-ct)], \quad H_0 \approx 4 K_0 d^2/3.$$

Since solitons have the unusual property of remaining undistorted after collision, the ensemble can be treated by linear superposition. The wavelength is taken as a random Poisson process and velocity vectors are taken to be uniformly distributed between $-\pi/2$ to $\pi/2$ in the downwind direction. The soliton spectrum can then be approximated as:

$$G_{2s} \approx \pi H^2 L^2/[1 + (KL/2)^2]^2$$

where H is rms elevation of the ensemble and L is the rms wavelength or the correlation length.

The soliton spectrum is simply added to the normal surface-wave spectrum and the backscattering strength is calculated by composite-surface theory.
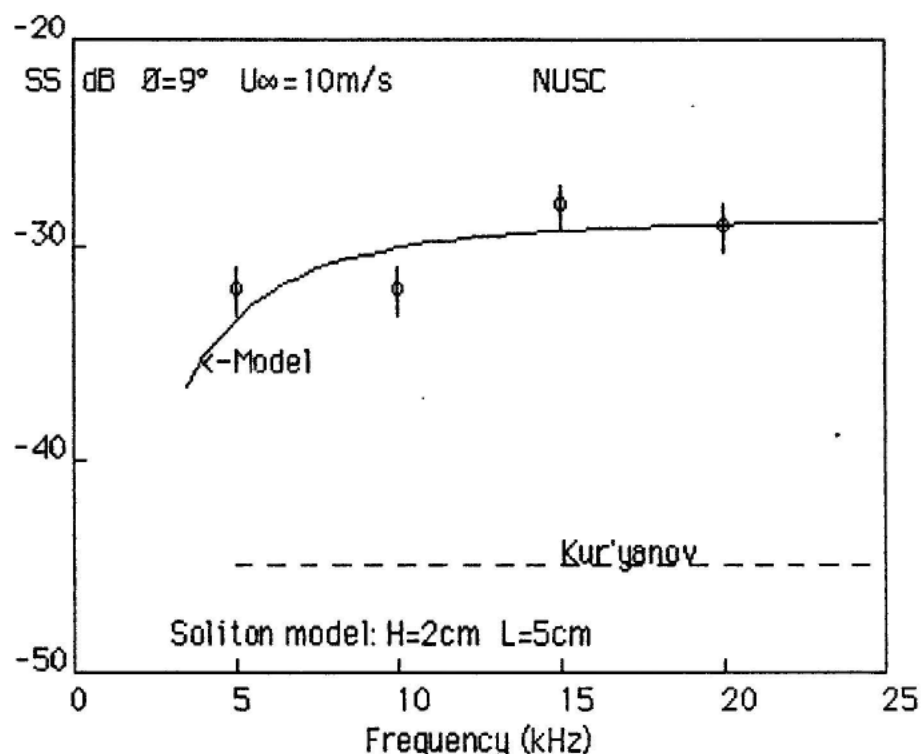
Figure 14: Experimental and model backscatter strengths (ref. 3).

Figure 14 compares "bubble-free" backscatter strength vs frequency for the model [1,2] with the experimental data of Roderick et. al. [3]. A soliton-ensemble of H=2 cm rms amplitude and an "effective" rms wavelength L= 5 cm has been included. The high-frequency surface-wave spectrum, however, is consistent with the measurements which show increasing levels at higher wind-speeds. Also shown is the predicted level for the composite two-scale scattering model of Kur'yanov [24], which is low by 15 dB. The added soliton component makes up the difference.

With two adjustable scaling parameters, there might appear to be much latitude in curve-fitting; however, the dependence on wind speed, or some related parameter, should be systematic. The soliton component can be expected to show critical threshold effects, i.e. vanishing for mean wind-speeds less than ~2m/sec. and saturating for speeds greater than ~10m/sec. However, mean wind-speed alone may not be an adequate parameter and the effects of gusts may also be important. Evidence for this is observed, not only in scattering, but also ambient noise. Both seem to show variations that are not strictly dependent on mean wind-speed.

- 14 -
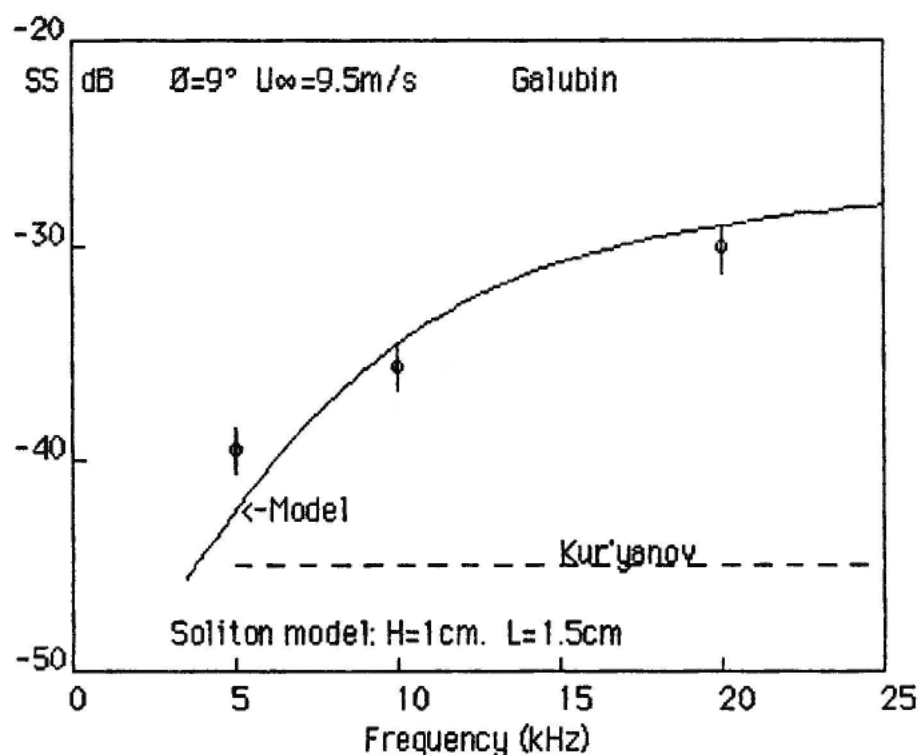
Figure 15: Experimental and model backscatter strengths (ref.8).

Figure 15 compares the model prediction with the experimental data of Galubin [8]. A soliton-ensemble of H=1 cm r.m.s amplitude and "effective" rms wavelength L=1.6 cm has been included. Also shown is the predicted level for the composite two-scale scattering model of Kur'yanov [24], which is in somewhat better agreement in this case, but still too low. The added soliton component, again, makes up the difference. Note that the surface roughness is evidently different from that of Figure 14 although the mean wind-speeds are nearly the same.

In order to check the plausibility of the model used in matching the backscattering data, it would be useful to have actual wavenumber spectra taken under similar wind conditions as the experiments. Unfortunately, only point frequency-spectra are available for this purpose. Furthermore, measurements made at sea, under appropriate conditions of wind and fetch, do not adequately cover the high-frequency region of concern. Therefore, laboratory point spectra of elevation will be used for comparison purposes.

Figure 16: Wave-flume frequency spectra (ref.17)

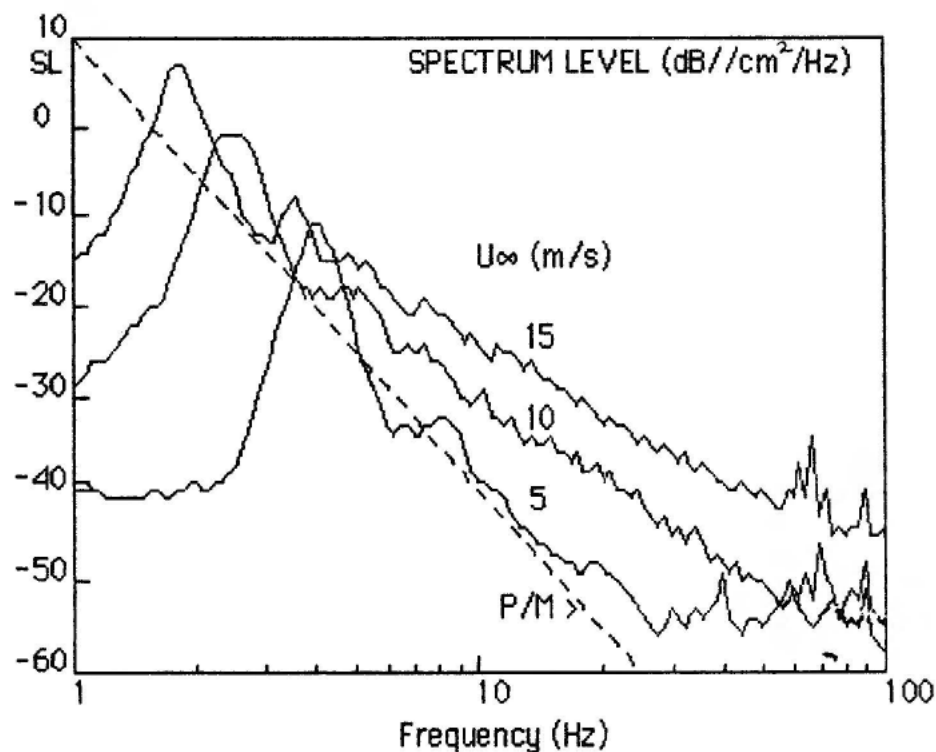Figure 16 shows wave elevation spectra measured in a wind-wave flume by Mitsuyasu and Honda [17] for 8.25 m fetch and mean wind velocities of 5, 10 and 15 m/s . The dashed line is the Pierson-Moskowitz [30] spectrum for the fully-developed equilibrium sea, which is given by:
$G(F)= 1 \times 10^{-5} \, g^2 \, F^{-5} \, \exp(-5 \times 10^{-4} g^4 \, F^{-4} \, U_\infty^{-4})$ where g is gravity, F is the frequency and U_∞ is mean wind-speed. Note that the P/M spectrum is saturated in the frequency range shown, its peaks falling well below 1 Hz. (e.g. at U∞=10 m/s the peak is at F≈0.14 Hz.) The data peaks do decrease in frequency with increasing wind-speed but the fetch is obviously far too small to approximate the fully-developed sea.

Transformation of the P/M asymptote to K-space using the gravity dispersion relation $K=(2\pi F)^2/g$ (neglecting azimuthal dependence) yields the asymptotic wavenumber spectrum $G_2(K)=1.5 \times 10^{-2} \, K^{-4}$.

At higher frequencies, the data fall well above the P/M asymptote and have roughly F^{-3} dependence. Without dispersion, $K=2\pi F/C$ where C is a constant and the spectral asymptote would also be K^{-4}.

The spectra also show several distinct peaks in the range 70-100 Hz, which may be due to the "capillary" ripples noted in Figure 11. Effects on scattering are significant only at 100 kHz or greater.

- 16 -
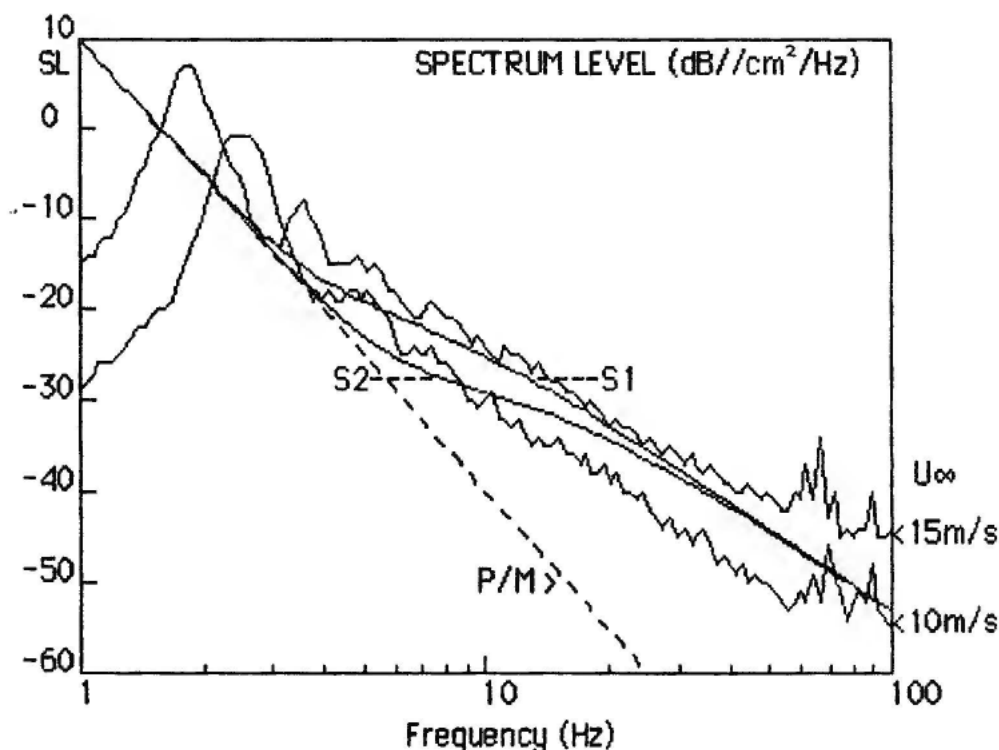
Figure 17: Wave frequency-spectra comparison.

Results are summarized in Figure 17. The curves labeled 10 and 15 m/s are the spectra of Figure 16. The curve P/M is the asymptotic Pierson-Moskowitz spectrum. The spectra S1 and S2 indicate addition of the respective soliton components used in Figures 14 and 15 to the P/M spectrum. The soliton components were calculated taking the propagation speed in the fixed-coordinate system to be 50 cm/s, which is in reasonable accord with measured values.

The wind-flume spectra have the same general shape as the model spectra; however, above 10 Hz, the 10 m/s wind-flume curve is lower than the model by as much 6 dB. This may not be too surprising in view of the very short fetch of the wind-flume experiment. In the backscattering experiments, fetches were of the order of kilometers. In the NUSC experiment, for example, the spectral peak occurred at 0.2 Hz, which is much closer to the calculated value.

The 15 m/s wind-flume spectrum is in much better agreement with the model, indicating that a higher wind-speed may tend to make up for the lack of fetch.

4. CONCLUSIONS

Models [1,2] based on soliton theory [14] describe essentially all of the known scattering phenomena at small grazing-angles and high frequencies in bubble-free regimes. By simply adding another component of roughness to the surface-wave spectrum, the theoretical backscattering strength and Doppler statistics all become consistent with experiment. Furthermore, the existence and behavior of the added component do not violate the known properties of the sea surface in any way. In fact, it appears to be a necessary condition on all counts.

The soliton hypothesis presented is a plausible mechanism for all the hydrodynamic phenomena involved. The evidence from scattering and wave-gauge measurements, points to specific characteristics of the small-scale roughness and the soliton appears to be the only kind of wave that can satisfy all requirements. The hydrodynamic effects are similar to water flowing down an inclined plane where nonlinearity causes the formation of hydraulic "bumps" with irregular wavefronts. On the sea surface, the velocities depend on local conditions of both the wind and the surface slope. Doppler shift reflects the mean speed in the downwind direction. The soliton hypothesis is consistent with Doppler measurements in detail. With reasonable physical assumptions relative to the soliton component, predictions of both spread and shift of the spectra can be put into very good agreement with experiment.

Wave-spectra, either measured or inferred from Doppler measurements, show no dispersion at high frequencies. The "dispersion" relation becomes $C \approx g/2\pi F$ for low frequencies (gravity regime) and $C \approx$ constant for high frequencies (nonlinear regime). The wavenumber spectra are then asymptotic to K^{-4} in both regimes. However, the spectrum levels can be much greater at high wavenumbers, depending on the wind conditions. The spectrum, therefore, tends to be saturated only in the low-wavenumber regime. Greater levels at high wavenumbers are required to explain the increase in scattering strength.

With the supporting evidence of the wave-gauge spectrum data, it seems clear that the extra roughness at high wavenumbers truly exists. From a theoretical standpoint, the soliton mechanism appears to be the only possible one. However a number of questions remain to be answered. Full justification of the model requires more detailed knowledge of both the parametric dependence on wind conditions as well as the hydrodynamics involved. The proposed experimental and theoretical investigations, outlined in the next section, should help to answer these questions.

5. PROPOSED RESEARCH PROGRAM OUTLINE

The problems with the experimental data reviewed in the previous sections are twofold:

1. Precise backscattering measurements have been made under conditions more or less typical of the open ocean; however, direct measurement of surface motion is very difficult under these conditions. As a consequence, direct evidence of the high-wavenumber properties of the surface are insufficient to validate the soliton model. We only know that the inferred properties are plausible and explain the observed acoustic phenomena whereas the conventional models do not.

2. Surface properties have been directly measured with some degree of accuracy and detail in the wind-wave flume experiments but only at very limited fetch. Corresponding scattering measurements have not yet been made under these circumstances.

Direct measurement of magnitude and dynamics of the small-scale surface roughness is absolutely essential, preferably under controlled ambient conditions. For example, apparent discrepencies in propagation speed were noted earlier and it would be a simple matter to discover if they are due to temperature. Surface properties can also be altered to find out the effects. At sea, it is evidently not possible to obtain the necessary data on surface fine-structure with presently available equipment and control of ambient conditions is much more limited.

Wind-flume experiments appear to be the most effective immediate avenue for continuing the investigation despite the fetch limitation. Conventional measurement methods can easily be extended to provide all the required data. Concurrent wave-gauge and backscatter measurements (both acoustic and radar), alone may be sufficient to reconcile the backscatter and surface-wave phenomena and provide the necessary information for extrapolation to sea conditions as well. In addition, with essentially the same instrumentation, it should be possible to obtain backscattering data from a controlled surface bubble-layer and thereby help resolve the controversy between "bubble" and "soliton" models.

A variety of experimental techniques can also be employed to measure surface properties with a precision not currently possible at sea. An array of wave-gauge sensors can serve to determine directional characteristics, propagation velocity and associated variability statistics. In addition, surface elevation in both dimensions can be measured using photographic and other image-display methods, e.g. Schlieren, holographic, and laser. Earlier experiments by Mellen (unreported), using a high-speed motion picture camera, showed the nonlinear steepening of ripples in a small tank. The surface-drift layer was also photographed using drops of dye.

Testing the soliton hypothesis against hydrodynamic theory would follow. When the properties of the rough sea-surfaces are known in more detail, it will be more feasible to attempt a quantitative description of the surface-dynamics and the parametric dependence on specific properties of the wind-flow.

Among the more immediate problems that need theoretical attention are:
1. Investigation of the various assumptions leading to expressions for covariance, spectra etc.
2. Development of results for the directional covariance and associated wavenumber and frequency spectra.
3. Investigate effects of soliton anisotropy on soliton statistics.
4. Modeling of decomposition of the complex surface into solitons and determining resulting statistics.
5. Analysis of proposed experiments under controlled conditions re. backscatter strength, Doppler shift and spread.
6. Modification and extension of the soliton model as indicated by experiment and hydrodynamical theory.
7. Analysis of backscattering measurements from bubble layers of known concentrations and size distributions to resolve the model controversy.

From the experimental evidence presented in this technical review, it seems clear that the proposed research program, outlined in this section, has far-reaching potential.

The primary aim, of course, is to understand the dynamics of the wind-driven sea surface as it relates to scattering. The soliton mechanism appears to be not only consistent with all the experimental evidence but also physically plausible in a qualitative sense. The proposed research will help to put it on a much more quantitative footing by demonstrating both magnitude and dependence on parameters of wind and water. The ultimate goal is to understand all aspects of wind-wave interaction; however, it would be a major advance simply to be able to predict scattering in detail from knowledge of certain critical parameters.

The relation of this study to the growth of wind-waves is serendipitous, the attempt to explain the observed scattering phenomena also revealing a potential generation mechanism. Energy exchange between wind and water, while crucial to understanding this phenomenon, remains a controversial subject. From the evidence, the proposed "chaotic" interaction process appears to be very promising. The proposed research program could answer certain critical questions and help point the way to a more comprehensive predictive model covering other aspects of sea-state development.
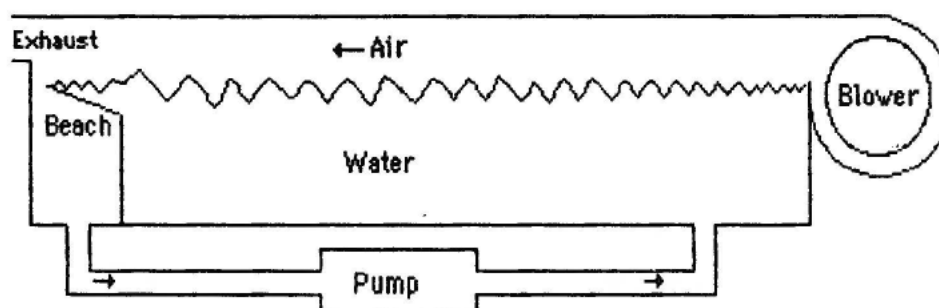
6. PROPOSED FACILITY

Figure 18. Typical wind-wave facility.

There are a number of tank facilities in existence; however, even if available, none seem to be suitable for present purposes. Wind-wave flume facilities may be adequate for wave generation purposes but are not suitable for acoustic measurements. Some of the acoustic facilities, on the other hand, may be of adequate size for scattering measurements but have inadequate wave-generation capability.

Figure 18 is a schematic section of a typical facility designed for wind-wave measurements. The blower on the right serves to generate the air flow which is confined by the top cover of the tank and exhausts at the left. The purpose of the "beach" is to prevent reflection of surface waves at the downwind end. Overflow water at the barrier is recirculated by pump.

In the wind-wave facility at the University of Karlsruhe [19], for example, the test section is 10.5 meters in length and the overall length is 24.5 m. The width and height of the flume are 1.8 and 1.2 m, respectively. The maximum water depth is 0.4 m. A centrifugal blower capable of generating 20 m/s air flow is employed.

The wave-generation capability of the Karlsruhe facility is perhaps comparable to that of the facilities in France [16] and Japan [17] and any of these designs might be adequate for wave-generating purposes; however, the shallow depth and lack of an anechoic lining would make acoustic measurements all but impossible. Backscattering measurements are need at wavelengths in the range 1-15 cm and this means acoustic frequencies as low as 10 kHz. Even using pulse methods, the wall reflections would make such measurements extremely difficult.

A wind-wave flume suitable for making surface-wave and scattering measurements would require somewhat larger dimensions of roughly 3 m depth, 4 m width and 25 m length and the blower requirement for 20 m/s air flow is then in the 100 HP range. To facilitate acoustic measurements, the inner below-water sides and bottom of the tank should be lined with anechoic wedges to reduce reflections. Conventional EM absorbing lining above the water-line would permit radar measurements.
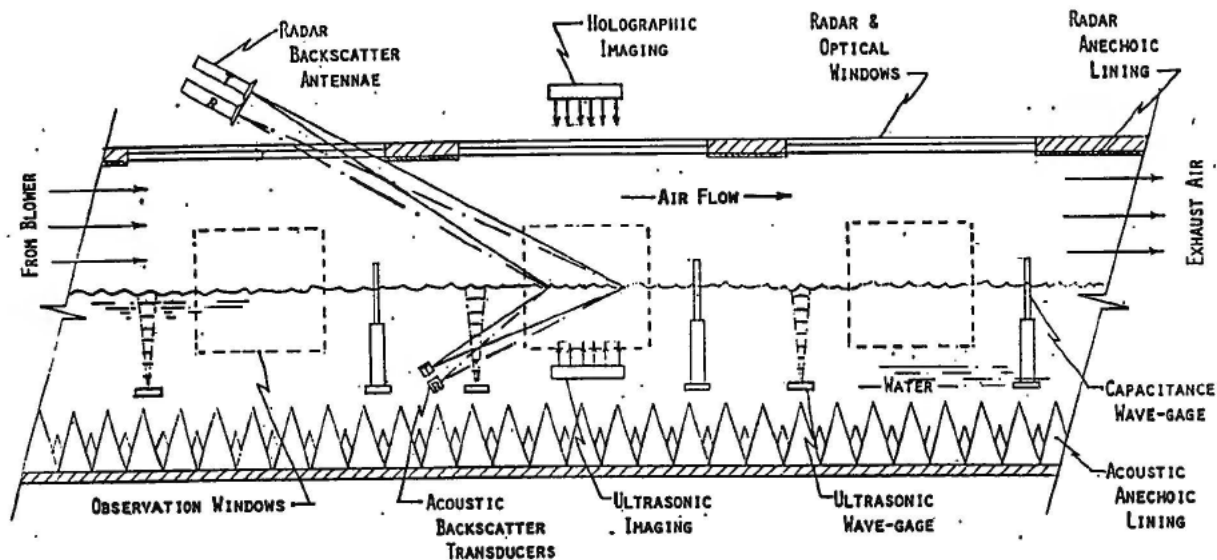

Figure 19. Sketch of proposed facility.

Figure 19 is a sketch of the proposed facility showing a portion of the test section with some of the anticipated instrumentation.

Acoustic transducers and radar antennae are arranged to illuminate a surface patch at selected grazing angles for backscatter measurements. For comparison purposes, the frequencies can be chosen to make the wavelengths equal; e.g. 3 cm for X-band EM and 50 kHz acoustic.

Capacitance wave-gauge arrays should be suitable for measuring the essential properties of the surface-wave; e.g. statistics, waveform, etc. as a function of wind speed and fetch; however, they will interfere with the scattering measurements. Ultrasonic arrays or imaging methods, either ultrasonic or holographic, would be an appropriate substitute when simultaneous backscatter and wave measurements of the same patch of water are desired.

Windows are also provided at the top and sides to allow monitoring the surface by visual observation as well as photographic and other optical methods, which are readily adaptable to the facility.

7. APPENDIX A

After the nonlinear wind-wave interactions have been sufficiently well-developed, the resulting surface wave distortions which ride on the thin drift-layer are described by ensembles of solitons of various magnitude and duration. These surface distortions are thus decomposable into a set of hydraulic "bumps" [4,5,31,32]. The thin drift-layer, of effective thickness d, provides the needed channel for the soliton creation and motion. From an analytical viewpoint, the soliton displacement h is represented by the limiting solutions another form of the Korteweg-de Vries (KdV) equation, which has been extended here to include the effects of surface tension T:

$$h_t + c_0[h_x + 3h\,h_x/2d + (d^2 - 3T/g)\,h_{xxx}/6] = 0$$

where $c_0 = (gd)^{1/2}$ and subscripts indicate derivation with respect to time t and space coordinate x. Dispersion (h_{xxx} term) is balanced by nonlinear steepening ($h\,h_x$ term), so that the solitons travel without change of shape. Surface-tension is included but viscosity is neglected. The limiting solution is a non-dispersive traveling wave with displacement given by:

$$h = d\,(8v_0/3c_0)^{1/2}\,\text{sech}^2[\,(3v_0/2c_0)^{1/2}(x - c\,t)/d],$$

where $c = v_0 + c_0$ and v_0 is the excess velocity relative to c_0. The gravity-capillary surface on which they ride is assumed to have the "normal" dispersion-relation $C^2 = g/K + T\,K$ where $K = 2\pi F/C$.
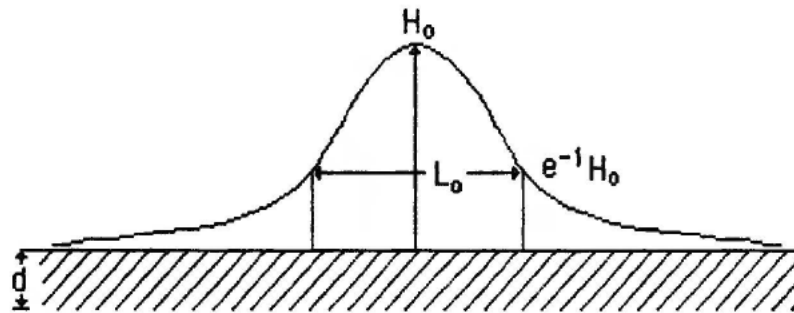
Figure 1A. Soliton cross-section.

A good approximation to the soliton solution is the Gaussian waveform shown in Figure 1A. For a soliton ensemble, it can be shown that [2,4,5]:

$$h(r,t) \approx \Sigma_j\,H_{0j}\,\exp[-4\,(\Delta r_j - c\Delta t_j)^2/L_{0j}^2]$$

where $L_{0j}^2 = (4d^2\,c_0/3v_0)_j$ and L_{0j} is the effective wavelength, which will be regarded as a random variable. The condition for true solitons to exist is $H_{0j}\,L_{0j}^2/d_j^3 > 32$. For smaller values, periodic "cnoidal" waves are generated (see [13], Eq. 100, p.466).

A reasonable probability density function (PDF) of wavelength L_0 is:

$$P(L_0) \approx (\pi L^2/2)^{-1/2} \exp(-L_0^2/2L^2) \quad L_0 \geq 0.$$

The temporal covariance for a random Poisson process is then [5]:

$$R(0,\Delta t) = H^2 \, |\beta| \, K_1(|\beta|) \qquad \beta = 2c_0 \Delta t/L$$

where K_1 is the modified Bessel function and H is the rms height and the vertical bars indicate absolute values. This result assumes that the propagation-speed is nearly constant, i.e. $c_j \approx c_0$.

The corresponding point intensity frequency spectrum of the soliton component is then given by:

$$G(F) \approx \pi H^2 L c_0^{-1}[1+(\pi F L/c_0)^2]^{-3/2}.$$

It can also be shown [5] that the directional covariance of the soliton ensemble can be expressed as:

$$R(\Delta r, \Delta t) = H^2 \langle |\beta'| \, K_1(|\beta'|) \rangle \quad \beta' = 2(c_0 \Delta t - \Delta r \cos\theta)/L$$

where $\langle \rangle$ indicates expectation values.

The spectrum of interest in calculating scattering strength is the wavenumber spectrum of the soliton field, which is given by:

$$G_2(K) \approx \pi H^2 L^2 [1 + (KL/2)^2]^{-2}$$

where L is the correlation length of the ensemble.

Various assumptions have been made to arrive at specific results [3], the scope and validity remaining to be investigated under the proposed research program:

1. Approximation of the exact solution of the KdV equation by the Gaussian form is a mathematical device to simplify the development.

2. The choice of the semi-Gaussian PDF for soliton wavelength L appears reasonable from the Central Limit Theorem argument. Moreover, it leads to wavenumber spectrum that has K^{-4} asymptotic dependence, which is consistent with experiment.

3. The soliton field is taken to be semi-isotropic and uniform in the downwind direction, i.e. $-\pi/2 \leq \theta \leq \pi/2$. For an isotropic gravity-wave component, this makes the scattering strength independent of azimuthal angle θ, but not the Doppler shift. Judging from experiment, this is probably a reasonably accurate model of actual anisotropic behavior, at least for the first approximation.

4. The soliton phase-speed is assumed constant. For the very small values of layer-thickness d, variations in amplitude tend to change L but not d.

5. Although H is proportional to v_0, it may be treated as effectively uncoupled from L by virtue of the soliton existence criterion. The scale of H depends, in part, on the actual decomposition of the local surface.
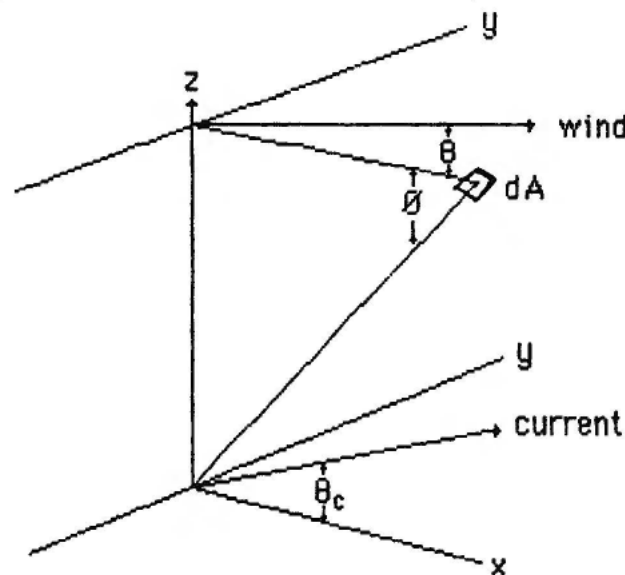
Figure 2A. Backscatter geometry.

The backscatter geometry is shown in Figure 2A. The illuminated area of the surface is dA, Ø is the grazing angle, θ is the azimuthal angle of the wind-vector and θ_c is the current azimuthal angle.

The backscattering strength SS can be shown to be given by [2]:
$$SS = R^2 \pi^{-1} N(\theta,\emptyset)\, k^4 H^2 L^2\, [1+ (k L \cos\emptyset)^2]^{-2}$$
where the wavenumber-resonance condition is $K = 2k \cos\emptyset$, k is the acoustic wavenumber, R is the effective reflectivity and $N(\theta,\emptyset)$ is the "tilt-factor". Shadowing effects can be neglected for Ø >5°; hence, $R \approx 1$. The effect of slopes of the large-scale wave components is included in the expression:
$$N(\theta,\emptyset) \approx 3s^4 \cos^4\emptyset + 6s^2\cos^2\emptyset \sin^2\emptyset + \sin^4\emptyset.$$
where s^2 is the effective variance of surface-slopes as determined by perturbation theory and conditions of the sea-surface model.

For present purposes, the gravity-wave will be assumed to be isotropic, i.e. independent of θ. In that case, the effective rms slope has been shown to be $s \approx S/16$ where S is the actual rms slope [1]. From the surface-glitter experiments of Cox and Munk [33], we have:
$$S^2 \approx (3+ 5.12\, U_\infty) \times 10^{-3}$$

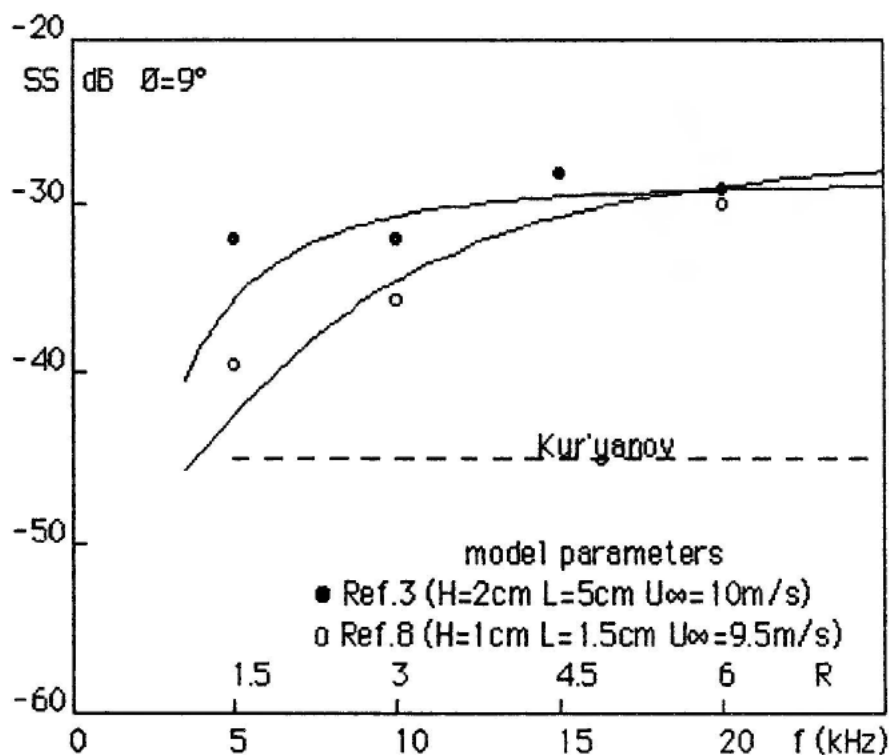where U_∞ is mean wind-speed in m/s.

- 25 -

Figure 3A. Backscatter strengths. (refs. 1,3,8)

Figure 3A compares the results of two recent experiments [3,8], with the theoretical estimates based on the conventional composite model [24] and the soliton-model [1,2]. The scattering theory is the Kirchhoff approximation, which remains valid for large values of the Rayleigh-roughness parameter, i.e. $R = kH \sin\emptyset > 1$. Note that a 2.5 dB Kirchhoff correction has been added to the soliton model to compensate for effects at small grazing-angles [1].

The values for the two experiments appear to be significantly different even though the mean wind-speeds were nearly the same. Narrow-band signals were used in Roderick's experiment [3} while Galubin [8] used explosives. Shock-wave effects at short range might be the cause of some error. However, in many other experiments, similar variability has been found with both methods of measurement. It is evident, therefore, that there can be distinct differences in surface roughness that are not simply a function of mean wind-speed. Fetch and wind duration are certainly important factors at the low-wavenumber end of the spectrum. Wind turbulence and current (both magnitude and direction) could have an effect at higher wavenumbers.
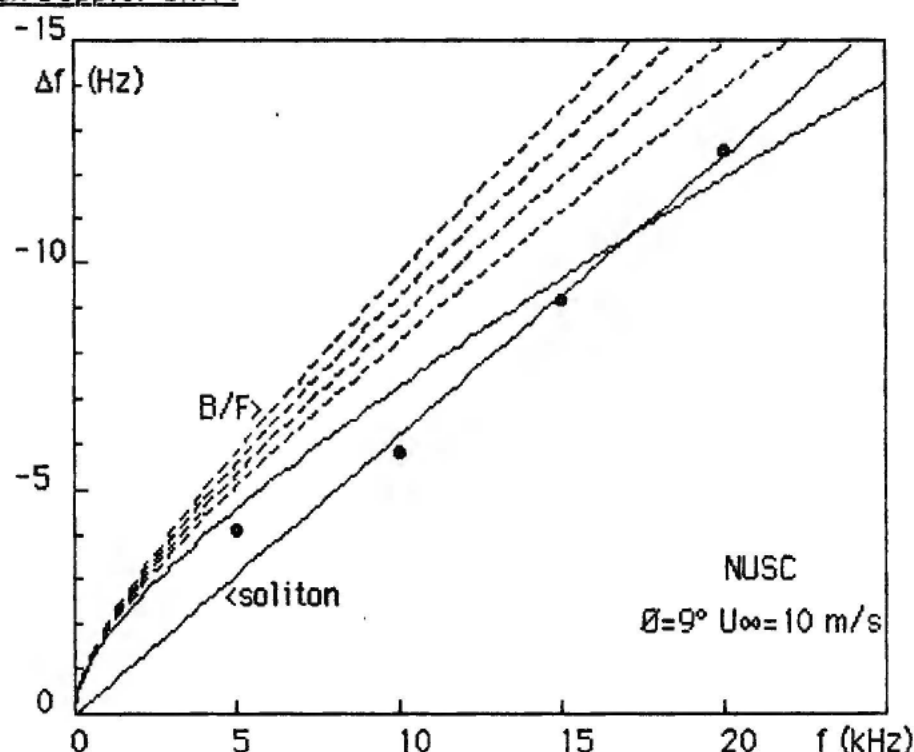
2A. <u>Mean Doppler Shift</u>

Figure 4A. Mean Doppler shift vs frequency. (ref.3)

Calculations for the classical B/F and soliton [2] models are compared with experimental data in Figure 4A. The theoretical expressions for mean Doppler-shift for the soliton and Bass and Fuks [34,35] models are:

$$\Delta f_{B/F} = (f\, g\, \cos\emptyset / \pi C_0)^{1/2} + 2f\, \cos\emptyset\, [U_0 \cos\theta + U_c \cos\theta_c]/C_0$$

$$\Delta f_S = 2f\, \cos\emptyset\, [(U_0 + c)\cos\theta + U_c \cos\theta_c]/C_0$$

where U_0 is the speed of the surface-drift, θ is the azimuthal angle, U_c is speed of the water current and θ_c is the current azimuthal angle as shown in Figure 2A. For the NUSC experiment, $\theta \approx 26°$, $U_c \approx 26$ cm/s and $\theta_c \approx 28°$. The solid B/F curve is the "classical" approximation. The dashed B/F curves include a correction for surface drift. The inferred soliton parameters for the corresponding values of drift-speed U_0 are listed below.

U_0(cm/s)	c_0(cm/s)	d (cm)	v_0 (cm/s)
10	17.7	3.2×10^{-1}	9.7×10^{-2}
15	13.2	1.8×10^{-1}	2.3×10^{-2}
20	8.7	7.7×10^{-2}	2.7×10^{-3}
25	4.2	1.8×10^{-3}	7.2×10^{-5}

- 27 -

3A Doppler Spread
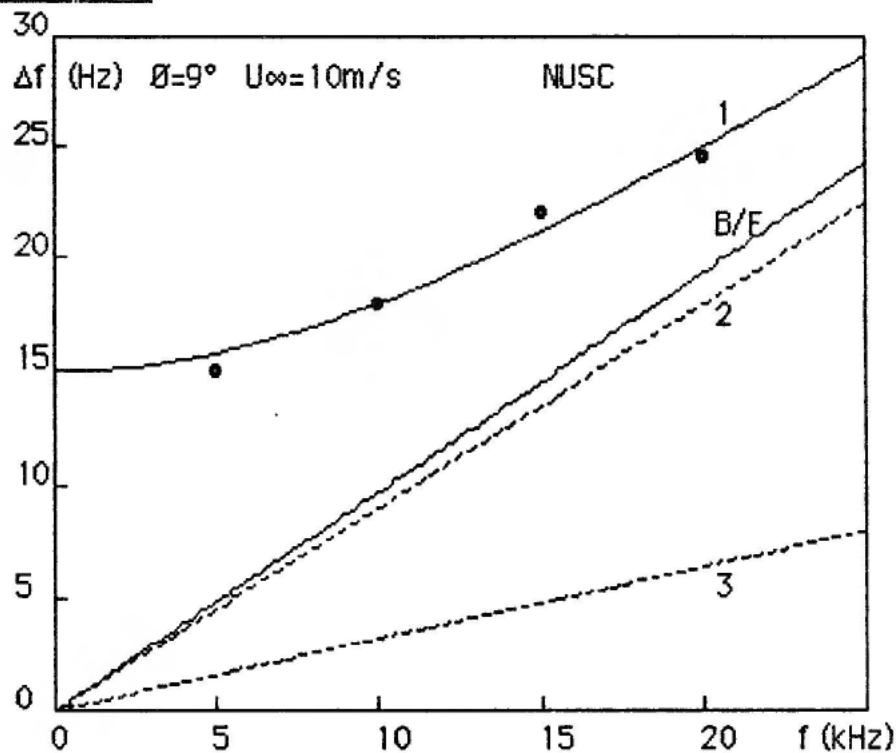

Figure 5A. Doppler spread vs frequency. (ref.3)

The Doppler spread for the two models are shown in Figure 5A. Spread is measured at the 1/e points of the spectrum.

The "classical" model B/F (solid line) [34,35] is given by $\underline{\Delta f}_{B/F} \approx 1 \times 10^{-3}\, f$.

The soliton model [2] (curve 1) is given by $\underline{\Delta f}_s \approx [(A^2 + B^2)\, f^2 + D^2]^{1/2}$

where the term A accounts for phase modulation by large-scale gravity waves, B accounts for the variations in soliton velocities and D is a frequency-independent random amplitude-modulation correction arising from variations in slope due to large-scale gravity waves. The data curve-fit values are: $A = 3.3 \times 10^{-4}$, $B = 7.8 \times 10^{-4}$ and $D = 15$. The dashed lines 2 and 3 show the effects for $D = 0$ and $B = D = 0$, respectively.

It is evident that, for small grazing angles and low frequencies, the soliton model ascribes most of the Doppler spread at to B and D. At larger angles, the phase-modulation term A becomes dominant and the two theories yield nearly the same values.

- 28 -

6. REFERENCES

1. D. Middleton, "Acoustic scattering cross-sections for truly composite wind-wave surfaces: I Scattering without bubbles", NUSC Tech. Doc. 7205, August 1984.

2. D. Middleton, "---: II Backscatter cross-sections and Doppler effects at high frequencies and small angles for 'bubble-free' regimes", NUSC Tech. Doc. (in publication)

3. W. I. Roderick, J. B. Chester and R. K. Dullea,"High-frequency acoustic backscatter from the sea surface", NUSC Tech. Doc. 7183, July 1984.

4. D. Middleton and R. H. Mellen,"Wind-generated solitons: a potentially significant mechanism in ocean surface wave generation and surface scattering", IEEE J. Oceanic Engineering $\underline{10}$*4. Oct. (1985).

5. D. Middleton, "Soliton mechanisms in wind-wave surface scattering: Underwater acoustic scatter models", NUSC Tech. Doc. (in publication)

6. R. H. Mellen and D. Middleton, "On the wind-wave interaction mechanism" presented at the Nashville ASA meeting, Nov. 1985.

7. L. Brekhovskikh and Yu. Lysanov, _Fundamentals of Underwater Acoustics_, (Springer-Verlag, New York 1982) Sec. 1.6

8. N. N. Galubin, "Back scattering of sound by a disturbed sea surface", Sov. Phys. Acoust. $\underline{22}$ 193-199 (1976)

9. S. T. McDaniel and A. D. Gorman, "Acoustic and radar sea-surface backscatter", J. Geophysical Res. $\underline{87}$ 4127-4136 (1982)

10. S. T. McDaniel and A. D. Gorman, "Examination of the composite-roughness scattering model", J. Acoust. Soc. Am. $\underline{73}$ 1476-1486 (1983)

11. G. P. deLoor, "Project Nordwijk, Part III: the radar backscatter coefficient as measured at Platform Nordwijk and comparison with other data", National Defense Research Organization TNO, The Hague, Netherlands, Report PHL 1982-22, May 1982.

12. R. T. Lawner and R. K. Moore, "Short gravity and capillary wave spectra from tower-based radar", IEEE J. Oceanic Eng. $\underline{OE-9}$ 317-324 (1984)

13. J. Lighthill, _Waves in Fluids_, (Cambridge University Press, 1979), pp. 463-468.

14. R. K. Dodd, J. C. Eilbeck, J. D. Gibbon and H. C. Morris, _Solitons and Nonlinear Wave Equations_, (Academic Press, New York 1982)

15. O. H. Shemdin,"Wind-generated current and phase speed of water waves", J. Phys. Oceanography, $\underline{2}$ 411-419 (1972)

16. A. Ramamonjiarisoa, S. Baldy and I. Choi,"Laboratory studies on windwave generation, amplification and evolution", in _Turbulent Fluxes Through The Sea Surface_, editors: A. Favre and K. Hasselmann (Plenum Press, New York 1978) pp.403-420

17. H. Mitsuyasu and T. Honda, "The high-frequency spectrum of wind-generated waves", J. Oceanographic Soc. Japan, $\underline{30}$, 185-198 (1974)

18. H. Mitsuyasu, "Measurement of the high-frequency spectrum of ocean wave surfaces", J. Phys. Oceanogr., 9, 882-891 (1977)

19. E. J. Plate, "Wind-generated water surface waves: the laboratory evidence" in Turbulent Fluxes Through The Sea Surface, editors: A. Favre and K. Hasselmann (Plenum Press, New York 1978) pp.385-401.

20. H. W. Marsh, "Sound reflection and scattering from the sea surface", J. Acoust. Soc. Am. 35 240-244 (1963)

21. O. M. Phillips, "The equilibrium range in the spectrum of wind-generated ocean waves", J. Fluid Mech. 4 426 (1958)

22. W. L. Konrad, D. G. Browning and R. H. Mellen, "Doppler spectra of sea-surface backscatter at high acoustic frequencies", NUSC Tech. Report 6735, July 1982.

23. R. J. Urick, Principles of Underwater Sound (McGraw-Hill, New York, 3d edition. 1983) Ch. 8, Fig. 8.18, p.264.

24. B. F. Kur'yanov,"The scattering of sound at a rough surface with two types of irregularity", Sov. Phys.-Acoust. 8, 252-257 (1963)

25. R. H. Mellen, "Doppler shift of sonar backscatter from the sea surface", J. Acoust. Soc. Am. 36, 1395-1396 (1964)

26. H. Boehme, "Measurements of acoustic backscattering from very rough water surfaces", J. Acoust. Soc. Am. 65, 350-359 (1979)

27. J. M. Wright and W. C. Keller, "Doppler spectra in microwave scattering from wind waves", J. Phys. Fluids 14, 466-474 (1971)

28. A. H. Schooley, "Profiles of wind-created water waves in the capillary-gravity transition region", J. Marine Res. 16 100-108 (1958)

29. M. L. Banner and O. M. Phillips, "On the incipient breaking of small scale waves", J. Fluid Mech. 65, 647-656 (1974)

30. W. L. Pierson Jr. and L. Moskowitz, "A proposed spectral form for fully-developed seas based on the similarity theory of S. A. Kitaigorodsky", J. Geophysical Res. 69 5180-5190 (1964)

31. G. E. Peterson, "Electrical transmission lines as models for soliton propagation in materials: Elementary aspects of video solitons", BSTJ 63 901-909 (1984)

32. M. Olsen, H. Smith and A. C. Scott, "Solitons in a wave tank", Am. J. Phys. 52 826-830 (1984)

33. C. S. Cox and W. H. Munk, "Measurement of the roughness of the sea surface from photographs of the sun's glitter", J. Opt. Soc. Am. 44 838-850 (1954)

34. F. G. Bass, I. M. Fuks, A. I. Kalnikov, I. E. Ostrovsky and A. D. Rosenberg, "Very high-frequency radiowave scattering by a disturbed sea surface" IEEE Trans. Antennas and Propagation, AP-16, 554-568 (1968)

35. F. G. Bass and I. M. Fuks, Wave Scattering from Statistically Rough Surfaces, (Pergamon Press, New York 1979)

INITIAL DISTRIBUTION LIST

Addressee	No. of Copies
ASN (RE&S)	1
OUSDR&E (Research & Advanced Technology)	1
Deputy USDR&E (Res & Adv Tech)	1
OASN, Director, Submarine & ASW Diagrams	1
ONR, ONR-102, -400, -410, -420, -422, -425, -425AC, Code 1125UA (Dr. R. Fitzgerald, R. Sternberg), 111 (Dr. T. Burlingcourt), 112 (G. Hamilton)	11
DIA, DT-2C	1
NRL, Code 5303 (Dr. L. Wetzel), Library	2
NORDA (Dr. R. Farwell, Dr. Ming-Yang Su, Dr. S. A. Chin-Bing, Library)	4
OCEANAV	1
NAVOCEANO	1
NAVELECSYSCOM, ELEX 304	1
NAVAIRDEVCEN	1
NOSC, Code 6565 (Library)	1
NAVSURFWPNCEN, Code U31	1
NAVPGSCOL (Prof. H. Medwin, Prof. C. Dunlap, Library)	3
APL/UW, SEATTLE	1
ARL/PENN STATE, STATE COLLEGE	1
DTIC	12
DARPA (A. Ellinthorpe)	1
ARL, UNIV OF TEXAS (Dr. H. Boehme, Prof. C. Horton, Library)	3
MARINE PHYSICAL LAB, SCRIPPS, (Library)	1
DIRECTOR SACLANT ASW RES CEN (Library, Dr. T. Akal, Dr. F. Jensen)	3
UNIV OF KANSAS (Dr. R. Lawner, R. Moore)	2
Dr. J. Brackett Hersey, Great Falls, VA	1
YALE UNIV (Prof. P. Schultheiss)	1
NOAA (Dr. S. Clifford)	1
UNIV OF WISCONSIN (Prof. S. Clay)	1
Dr. D. Middleton, New York, NY	10
SONALYSTS, INC. (W. Pugliese)	1
RSMAS Applied Marine Physics, UNIV OF MIAMI (Prof. F. Tappert, Prof. H. Ferrari)	2
MIT E34-458 (Dr. G. Duckworth)	1
FWG, Klausdorfer Weg 2-24 (Dr. H. Schneider, Dr. P. C. Wille)	2
SACLANTCEN (Library, Dr. T. Akal, Dr. F. Jensen)	3
JOHNS HOPKINS UNIV. (Prof. O. Phillips)	1
MIT, Cambridge MA (Prof. E. Mollo-Christensen)	1
Jet Propulsion Lab. CIT (Dr. O. Shemdin)	1
City College of New York (Prof. W. Pierson)	1
National Water Research Institute, Ontario, Canada (Dr. M. Donelan)	1
Institut de Mechanique Statistique de la Turbulence, Marseilles, France (Dr. A. Favre, Dr. A. Ramamonjiarisoa)	2
Research Institute for Applied Mechanics, Japan (Prof. H. Mitsuyasu)	1

INITIAL DISTRIBUTION LIST (Cont'd)

Addressee	No. of Copies
Dept of Applied Mathematics and Theoretical Physics, Cambridge, UK (Prof. M. S. Longuet-Higgins)	1
Meteorological Institute, University of Hamburg (Prof. D. Hasselmann)	1
Defense Scientific Establishment, Auckland, New Zealand (Library, Dr. K. M. Guthrie)	2
Royal Australian Navy Research Laboratory (Library, Dr. M. Hall)	2
Servicio Naval de Investigacion y Desararrolo, Buenos Aires, Argentina (Prof. J. C. Novarini)	1
Industrial Acoustics Laboratory, Technical University of Denmark (Prof. L. Björnö)	1
Woods Hole Oceanographic Institution (Library)	1
Institute of Geophysics and Planetary Physics, University of California (Dr. W. Munk)	
Defence Research Establishment Atlantic (Library, Dr. H. Merklinger)	2
Defense Research Establishment Pacific (Library, Dr. R. Chapman, Dr. D. Thomson)	3
ARL/PENN STATE, STATE COLLEGE (Library, Dr. S. McDaniel)	2
Norwegian Defence Research Establishment KJV, Norway (Library, Dr. I. Engelsen)	2